Acta Crystallographica Section D
Biological Crystallography
ISSN 0907-4449

Structure of the carboxy-terminal PH domain of pleckstrin at 2.1 Å

S. G. Jackson,[a] Y. Zhang,[b] X. Bao,[b] K. Zhang,[a] R. Summerfield,[a] R. J. Haslam[a,b] and M. S. Junop[a]*

[a]Department of Biochemistry and Biomedical Sciences, McMaster University, Canada, and [b]Department of Pathology and Molecular Medicine, McMaster University, Canada

Correspondence e-mail: junopm@mcmaster.ca

Received 30 September 2005
Accepted 23 December 2005

PDB Reference: pleckstrin C-terminal PH domain, 1zm0, r1zm0sf.

Pleckstrin is an important intracellular protein involved in the phosphoinositide-signalling pathways of platelet activation. This protein contains both N- and C-terminal pleckstrin-homology (PH) domains (N-PH and C-PH). The crystal structure of C-PH was solved by molecular replacement and refined at 2.1 Å resolution. Two molecules were observed within the asymmetric unit and it is proposed that the resulting dimer interface could contribute to the previously observed oligomerization of pleckstrin in resting platelets. Structural comparisons between the phosphoinositide-binding loops of the C-PH crystal structure and the PH domains of DAPP1 and TAPP1, the N-terminal PH domain of pleckstrin and a recently described solution structure of C-PH are presented and discussed.

1. Introduction

Pleckstrin was first identified as a phosphorylated protein in the cytosol of activated platelets (Lyons *et al.*, 1975; Haslam & Lynham, 1977). It is exclusively expressed in haematopoietic cells of myeloid and lymphoid origin (Tyers *et al.*, 1987; Gailani *et al.*, 1990), where it serves as the major substrate of protein kinase C (Sano *et al.*, 1983). After cloning of pleckstrin as a 350-amino-acid protein, N- and C-terminal regions of about 100 residues were identified as having significant primary sequence identity and similarity (Tyers *et al.*, 1988, 1989). Subsequently, the presence of related sequences was detected in a wide variety of other proteins involved in signal transduction and cytoskeletal regulation (Haslam *et al.*, 1993; Mayer *et al.*, 1993). These regions were termed pleckstrin-homology (PH) domains. An intermediate DEP domain was also identified (named after the proteins dishevelled, egl-1 and pleckstrin; Ponting & Bork, 1996). The first clue as to the role of PH domains came with the discovery that the pleckstrin N-terminal PH domain (N-PH) and the C-PH domain could bind to phosphatidylinositol 4,5-bisphosphate [PtdIns(4,5)P_2; Harlan *et al.*, 1994], although subsequent studies showed that C-PH has a much higher affinity for PtdIns(3,4)P_2 (Zhang *et al.*, 2003; Edlich *et al.*, 2005).

Although thought to be important for intracellular signalling, the exact role of pleckstrin within platelets remains unclear. Some studies have suggested that phosphopleckstrin may inhibit phosphoinositide metabolism by PLCβ and PLCγ (Abrams, Wu *et al.*, 1995) and by PI3Kγ (Abrams, Zhang *et al.*, 1996). However, this work is based upon overexpression of pleckstrin in COS-1 and HEK-293 cells and there is no evidence that such inhibition occurs in intact platelets. Perhaps more significantly, pleckstrin has been found to associate with the $\beta\gamma$ subunit of G-proteins (Abrams, Zhao *et al.*, 1996). In addition, phosphopleckstrin associates with

inositol 5-phosphatase I in platelet cytosol to activate the hydrolysis of the inositol phosphates Ins(1,4,5)P_3 and Ins(1,3,4,5)P_4, thereby functioning to terminate Ca^{2+} signalling (Auethavekiat *et al.*, 1997). Pleckstrin has also been linked to changes in cell morphology. Expression of wild-type pleckstrin in Cos-1 cells induced the formation of actin microspikes and membrane ruffles, a process dependent on its N-terminal PH domain and the small G-protein Rac (Ma & Abrams, 1999). A link between pleckstrin and integrin $\alpha_{IIb}\beta_3$ was also found to be responsible for phosphopleckstrin-mediated cell spreading in REF52 and CHO cells (Roll *et al.*, 2000).

Nonphosphorylated pleckstrin appears to be oligomerized in resting platelets, but after phosphorylation only the monomeric form can be detected in cross-linking experiments (Imaoka *et al.*, 1983; McDermott & Haslam, 1996). Phosphorylation of pleckstrin on Ser113, Thr114 and Ser117 by PKC (Abrams, Zhao *et al.*, 1995; Craig & Harley, 1996) may prevent self-association of the protein and thus regulate interactions of the protein with its ligands (McDermott & Haslam, 1996; Sloan *et al.*, 2002).

Although PH domains were originally found to bind to membrane phosphoinositides (Harlan *et al.*, 1994), only a small number of PH domains, in proteins such as PLC δ1, Akt and TAPP1, have been shown to have a high affinity and specificity for particular phosphoinositides (Lemmon, 2003). In addition to their ability to mediate membrane localization by phosphoinositide binding, PH domains may also act to regulate protein function by facilitating protein–protein interactions. PH domains are therefore thought to be involved in regulating multiple aspects of intracellular signalling (reviewed in Cozier *et al.*, 2004).

NMR structures are now available for each of the three domains of pleckstrin (Yoon *et al.*, 1994, PDB code 1pls; Civera *et al.*, 2005, PDB code 1w4m; Edlich *et al.*, 2005, PDB code 1xxo). Here, we report the X-ray crystal structure of the carboxy-terminal PH domain (C-PH) of human pleckstrin determined at 2.1 Å resolution. Structural comparisons with the PH domain of DAPP1, the N-PH domain of pleckstrin, the C-terminal PH domain of TAPP1 and with the recently reported solution structure of the C-PH domain of pleckstrin (Edlich *et al.*, 2005; PDB code 1xxo) are presented. In addition, we report the identification of a dimer interface that could help to mediate pleckstrin oligomerization. The functional relevance of amino acids previously implicated in phosphoinositide binding are also discussed.

2. Materials and methods

2.1. Protein expression and purification

The carboxy-terminal PH domain (amino acids 240–350) of human pleckstrin was expressed and purified as a glutathione *S*-transferase (GST) fusion protein in *Escherichia coli* BL21(DE3) cells using the pGEX-4T-1 expression vector (Amersham-Pharmacia Canada Ltd). Cells were grown at 310 K with shaking (220 rev min^{-1}) in LB medium supplemented with 50 µg ml^{-1} ampicillin until the light absorbance at 600 nm reached 0.5. Protein expression was then induced with 0.2 m*M* IPTG and the incubation temperature was decreased to 303 K. After an additional 4 h, the bacteria were harvested. Clarified cell lysate containing the GST-tagged C-PH protein was first purified using glutathione-Sepharose according to the manufacturer's instructions (Amersham-Pharmacia Canada Ltd). Following on-column thrombin treatment (100 U ml^{-1}) at 277 K overnight in phosphate-buffered saline (PBS), the C-PH domain of pleckstrin was isolated as unbound protein. Thrombin was subsequently removed by passing the mixture over a 0.5 ml column containing *p*-aminobenzamidine agarose (Sigma) that had been washed sequentially with 10 m*M* benzamidine in PBS (ten bed volumes) and PBS. Any remaining protease was inactivated with 1 m*M* PMSF. The resulting protein was concentrated to 5.0 mg ml^{-1} as determined by the Bradford assay. SDS–PAGE analysis indicated that C-PH protein purity was greater then 95%. C-PH domain prepared by this method contains an additional three amino-acid residues (GSP) at the N-terminal end derived from the thrombin cleavage site.

2.2. Crystallization and data collection

Crystallization was carried out using the hanging-drop vapour-diffusion method. Crystals were grown at 297 K using the following conditions. A 4 µl drop containing 2 µl 5.0 mg ml^{-1} C-PH domain in 25 m*M* HEPES buffer pH 7.4 with 100 m*M* NaCl, 1 m*M* EDTA, 1 m*M* DTT, 1 m*M* benzamidine and one protease-inhibitor cocktail tablet (Roche Diagnostics) was mixed with 2 µl of mother liquor containing 0.1 *M* Tris buffer pH 8.9, 0.05 *M* magnesium acetate and 6% glycerol. Rectangular rod-shaped crystals grew to final dimensions of 500 × 150 × 150 µm after a 4–6 d incubation period. Prior to cryocooling in a nitrogen cold stream, the crystals were soaked briefly (<30 s) in a cryoprotectant solution containing 0.1 *M* Tris pH 8.9, 0.05 m*M* magnesium acetate and 30% glycerol. Two X-ray diffraction data sets were collected. The first data set, used for structure determination *via* molecular replacement, was collected to 2.7 Å at beamline 17-ID of the Advanced Photon Source at the Argonne National Laboratory. Data were collected at a wavelength of 0.9785 Å using an ADSC Quantum 210 CCD detector. This data set was processed using *d*TREK* (Pflugrath, 1999). A second higher resolution data set, used for final model refinement, was collected to 2.1 Å at a home source equipped with an R-AXIS IV image-plate detector mounted on an RU300 rotating-anode X-ray generator (Rigaku). This higher resolution data was indexed and scaled using *DENZO* and *SCALEPACK* (Otwinowski & Minor, 1997).

2.3. Structure determination and model refinement

The structure of C-PH was solved by molecular replacement using a highly redundant lower resolution data set and the program *MOLREP* (Vagin & Teplyakov, 1997). The search model used in molecular replacement was based on the crystal structure of the PH domain from DAPP1 (Ferguson *et al.*,

Table 1
Crystallographic data and refinement statistics.

Data for the highest resolution shell are shown in parentheses.

	Data set 1	Data set 2
Data collection		
Space group	$P4_12_12$	$P4_12_12$
Unit-cell parameters (Å, °)	$a = b = 54.9$, $c = 148.3$, $\alpha = \beta = \gamma = 90$	$a = b = 54.6$, $c = 148.2$, $\alpha = \beta = \gamma = 90$
No. of molecules in ASU	2	2
Resolution range (Å)	44.16–2.7 (2.8–2.7)	50.0–2.1 (2.14–2.10)
Unique reflections	6927	13029
Data redundancy	13.03 (13.46)	3.37 (1.89)
Completeness (%)	100 (98.4)	84.2 (70.5)
$I/\sigma(I)$	16.5 (5.0)	24.5 (3.2)
R_{merge} (%)	8.3 (47.7)	5.0 (14.7)
Model and refinement		
Resolution range (Å)		50.0–2.1 (2.14–2.10)
R_{work} (%)		23.6
R_{free} (%)		24.5
No. of reflections		12111 (11197 in working set, 914 in test set)
Cutoff criterion		$\|F\|/\sigma(F) > 2.5$
No. of amino-acid residues/atoms		194/1564
No. of waters		175
R.m.s.d. bond lengths (Å)		0.012
R.m.s.d. bond angles (°)		1.9
Average B factor (Å^2)		50.1

2000; PDB code 1fb8). The search model was constructed manually by combining C^{α} coordinates from the DAPP1 PH domain structure with modelled pleckstrin C-PH side chains. Amino acids from pleckstrin corresponding to the following regions were removed from the search model to generate the final search model used in molecular replacement: Gly255–Asn260, Glu270–Tyr274, Asp279–Leu287, Glu301–Asn313 and Thr310–Val323. Model refinement was carried out using a second data set collected to 2.1 Å. Iterative cycles of manual model building and refinement were carried out using the programs *O* (Jones *et al.*, 1991) and *CNS* (Brünger *et al.*, 1998), respectively. The final model contains two C-PH monomers in the asymmetric unit. The first three C-PH amino-terminal residues and the last three carboxy-terminal residues in the first monomer and the first two amino-terminal residues and last three carboxy-terminal residues in the second monomer were excluded from the final model owing to poor electron density. In addition, residues 301–311 and 301–309 are missing in monomers *A* and *B*, respectively. Analysis of the Ramachandran plot calculated by *PROCHECK* (Laskowski *et al.*, 1993) indicated that 90.4% of the residues in the final model are in the most favoured regions, with the remaining 9.6% of the residues located in the allowed regions. Crystallographic data and final refinement statistics can be found in Table 1. All figures presented were generated using the *PyMol* molecular-graphics system (DeLano, 2002).

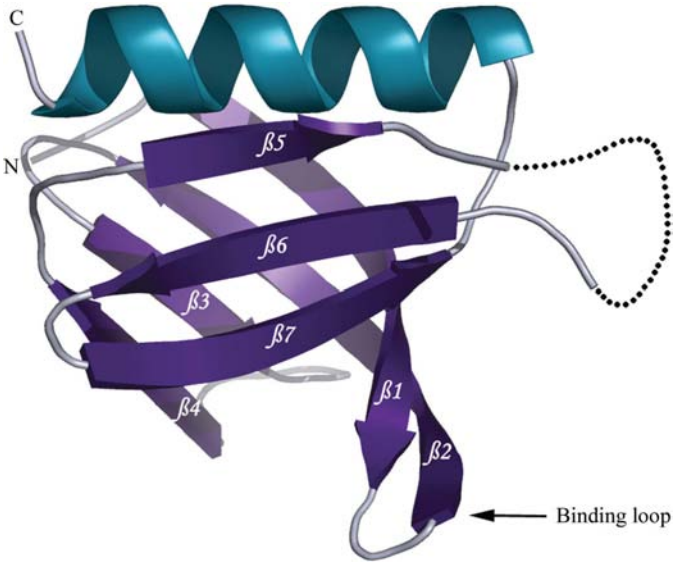

Figure 1
Ribbon diagram of the C-PH domain. β-Strands coloured in purple are labelled sequentially, $\beta1$–$\beta7$, and the single C-terminal α-helix is shown in cyan. The disordered loop between the fifth and sixth β-strands is represented by a broken line. The phosphoinositide-binding loop is indicated with an arrow.

3. Results and discussion

3.1. Overall structure of the pleckstrin C-PH domain

The crystal structure of the carboxy-terminal PH domain of pleckstrin (Fig. 1) was determined by molecular replacement and refined to 2.1 Å (Table 1). Other than the $\beta5$–$\beta6$ loop corresponding to residues 301–311, the electron density for the entire molecule was very clear and continuous. The overall fold of the C-PH is similar to the general architecture observed for other PH-domain structures (Cozier *et al.*, 2004). As shown in Fig. 1, the C-PH domain is comprised of a seven-stranded antiparallel β-sandwich derived from two β-sheets, one with three β-strands and the second with four β-strands. A carboxy-terminal α-helix closes one end of the β-sandwich, while the other end remains open. During the final stages of refinement of this structure, the solution structure of the carboxy-terminal PH domain of pleckstrin was reported (Edlich *et al.*, 2005; PDB code 1xxo). The solution and crystal structures of the C-PH are in good general agreement with each other, with an overall r.m.s.d. of 1.02 Å.

The flexibility we observed in the $\beta5$–$\beta6$ loop region is consistent with ^{15}N relaxation studies conducted by Edlich *et al.* (2005), which also indicated that this region of the C-PH adopts an unstructured conformation. As there are no reports in the literature implicating the C-PH $\beta5$–$\beta6$ loop in phosphoinositide binding, the function and relevance of its flexibility remain uncertain. Perhaps this loop adopts a more ordered conformation upon making interactions with other pleckstrin domains or potentially with distinct proteins not yet identified as pleckstrin binding partners. Interestingly, the $\beta5$–$\beta6$ loop contains a net positive charge and resides on the same surface of the C-PH as the $\beta1$–$\beta2$ loop (Fig. 1), suggesting that this loop may play a role in further stabilizing pleckstrin–membrane binding *via* non-specific interactions with negatively charged lipid head groups.

3.2. C-PH dimerization

Although native pleckstrin has been shown to exist as dimers and higher oligomers prior to but not after its phosphorylation, the interface responsible for mediating this oligomerization has not been determined (McDermott & Haslam, 1996). Two molecules of the C-PH domain were observed within the asymmetric unit of the crystal structure reported here (Fig. 2). The dimer interface between non-crystallographically related monomers of C-PH results from the burying of surface located reciprocally between the carboxy-terminal α-helix of one monomer and the fifth β-strand of the other. At 1124 Å^2, the resulting buried surface is comparable to other proteins known to form stable interactions, which typically bury between 1200 and 2000 Å^2 (Janin & Chothia, 1990). Although NMR has been successful in providing structural information for each of the three domains of pleckstrin (Yoon *et al.*, 1994, PDB code 1pls; Civera *et al.*, 2005, PDB code 1w4m; Edlich *et al.*, 200, PDB code 1xxo), no evidence has previously been reported to suggest which region of the protein could be responsible for mediating oligomerization. However, in the absence of structural information for full-length pleckstrin, it is difficult to predict how much of the entire pleckstrin dimer interface is accounted for by the C-PH dimer interface reported here.

3.3. Phosphoinositide binding

The phosphoinositide-binding pocket of C-PH is located in the loop region between the β1 and β2 strands (Fig. 3) and has been shown to be selective for phosphatidylinositol-3,4-bisphosphate [PtdIns(3,4)P_2] in experiments with phosphatidylcholine liposomes containing specific 3-phosphoinositides (Zhang *et al.*, 2003; Zhang, 2005) or in protein–lipid overlay assays (Edlich *et al.*, 2005). The former but not the latter study also showed that C-PH binds PtdIns(3,4,5)P_3, although less firmly. The reason for this discrepancy is presumably methodological. NMR titration studies performed by Edlich *et al.* (2005) identified amino acids Lys253, Arg257, Arg258, Lys259, Lys262 and Arg264 as key components of the C-PH phosphoinositide-binding pocket. This work was complemented by mutation studies, which demonstrated that the mutations K253N, H256G, R257N, R258N, K262N and Y277F all independently abolished binding to PtdIns(3,4)P_2 (Edlich *et al.*, 2005). Fig. 3 shows the relative positions of these residues as observed within the NMR and crystal structures. While some of these amino acids (Lys253, Lys262 and Arg264) reside in similar positions, others including His256, Arg257, Arg258 and Lys259 do not. These differences, while significant, may reflect the fact that both structures were determined in the absence of ligand. Nevertheless, all of these residues in both structures are orientated in a similar direction, forming a positively charged cleft on one face of the β1–β2 loop, the only

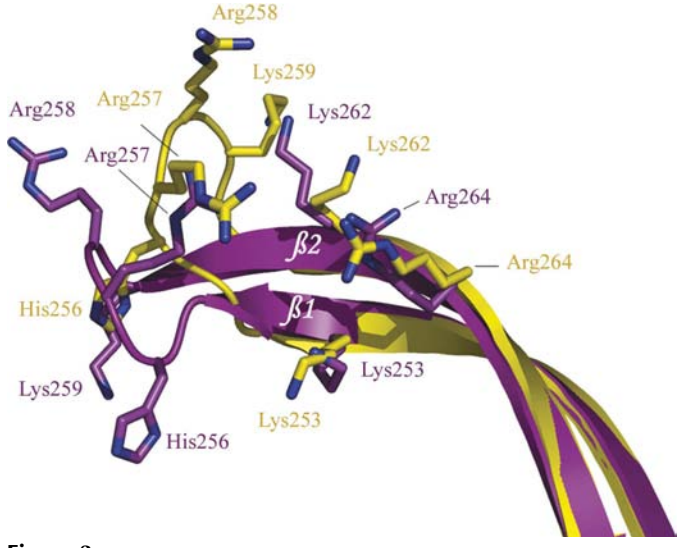

Figure 3
Structural superimposition of the solution and crystal structures of C-PH. The NMR (yellow) and crystal (purple) structures are represented in a combined stick and ribbon diagram.

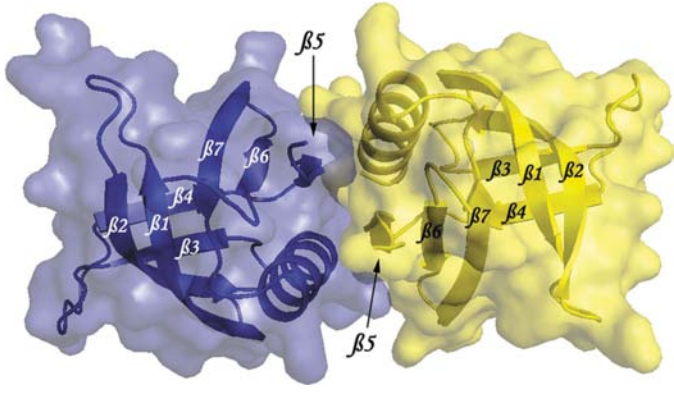

Figure 2
The observed non-crystallographic C-PH dimer. The dimer interface is illustrated using a combination of ribbon and semi-transparent space-filling diagrams. A reciprocal interaction between the fifth β-strand from one subunit and the α-helix from the other forms the dimer interface. Subunits *A* and *B* are coloured blue and yellow, respectively.

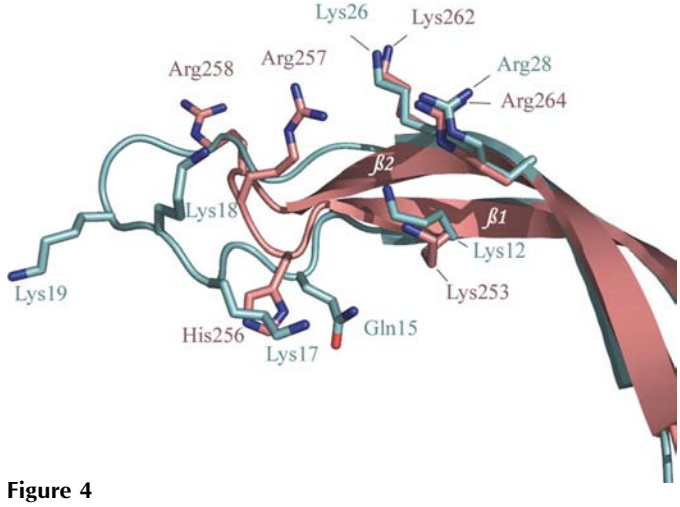

Figure 4
Structural superimposition of the Btk PH domain with C-PH. The Btk PH domain and C-PH are coloured cyan and salmon, respectively. Residues Lys12, Lys17, Lys18, Lys19, Lys26 and Arg28 of the Btk PH domain are comparable to Lys253, His256, Arg257, Arg258, Lys262 and Arg264 in C-PH.

exception being Lys259 in the crystal structure, which points away from this region.

Interestingly, in the mutation studies performed by Edlich *et al.* (2005), Arg264 was not tested despite being identified as a key component of the phosphoinositide-binding pocket. This arginine residue is conserved amongst a number of PH domains, in particular that of Bruton's tyrosine kinase (Btk) (Arg28), where substitution to either proline or histidine has been shown to cause the hereditary immune disease X-linked agammaglobulinaemia (XLA; Smith *et al.*, 1994). In the crystal structure of the PH domain of Btk complexed with inositol 1,3,4,5-tetrakisphosphate [Ins(1,3,4,5)P_4], it was observed that the side chain of this arginine residue contacts the 3-phosphate through two hydrogen bonds and consequently mutation of this arginine is thought to cause XLA by decreasing the affinity of the PH domain for its natural ligand, PtdIns(3,4,5)P_3 (Baraldi *et al.*, 1999; PDB code 1b55). Comparison of the crystal structures of the wild-type and R28C mutant PH domains of Btk reveals that this mutation causes a conformational change in the $\beta1$–$\beta2$ loop where ligand binding occurs (Baraldi *et al.*, 1999). In addition, binding studies conducted with the C-PH domain of pleckstrin showed that mutation of arginine at position 264 abolished binding to PtdIns(3,4)P_2 (Zhang *et al.*, 2003; Zhang, 2005). A structural alignment of the Btk PH domain with C-PH of pleckstrin indicates that the position of this arginine residue is highly conserved between these proteins (Fig. 4). Therefore, it seems reasonable that this conserved arginine would play an important role in binding to PtdIns(3,4)P_2.

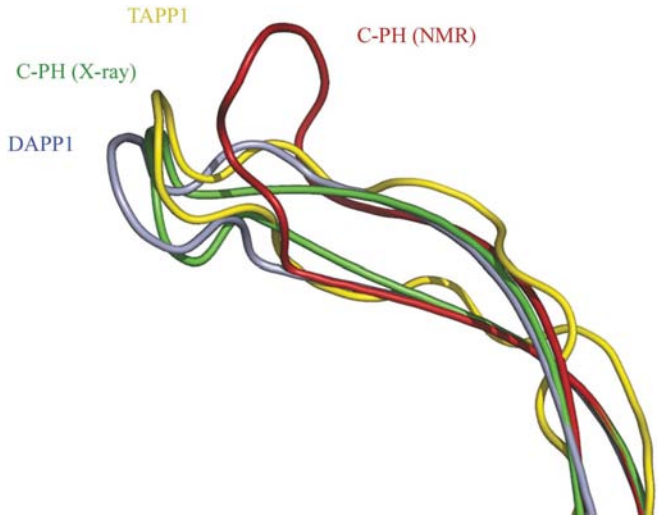

Figure 5
Structural comparison of the phosphoinositide-binding loops from the PH domains of TAPP1 (C-terminal), DAPP1, C-PH (X-ray) and C-PH (NMR). Cartoon-loop representations of the PH domains of TAPP1 (C-terminal), DAPP1, C-PH (X-ray) and C-PH (NMR) are coloured yellow, blue, green and red, respectively.

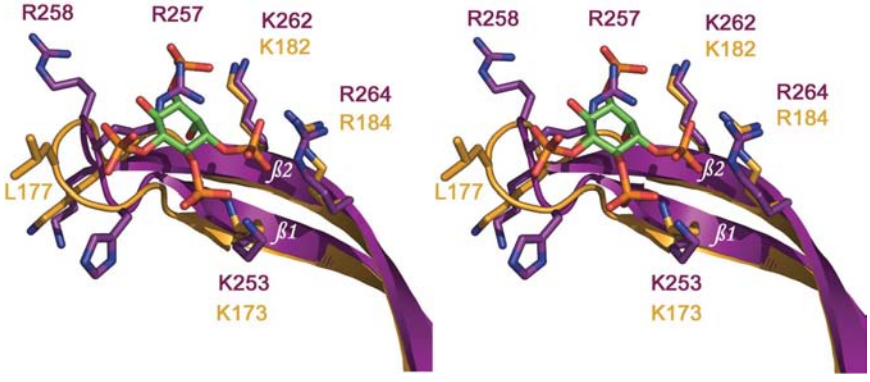

Figure 6
Stereoview of the structural comparison between the DAPP1 PH and C-PH ligand-binding pockets. DAPP1 PH is shown in gold using a combined ribbon/stick representation, while C-PH is shown in purple. Ins(1,3,4,5)P_4 observed in the DAPP1 structure is shown with C atoms in green, phosphate in orange and O atoms in red.

The C-PH domain of pleckstrin is most similar in terms of sequence similarity and binding specificity to the PH domains of TAPP1 (C-terminal) and DAPP1. Fig. 5 compares the general conformation of the $\beta1$–$\beta2$ binding loops from these structures, as well as those of the C-PH domain of pleckstrin determined by X-ray crystallography (this study) and NMR (Edlich *et al.*, 2005). With the exception of the C-PH NMR structure, the $\beta1$–$\beta2$ loops all adopted very similar conformations. The conformation of the $\beta1$–$\beta2$ loop in the crystal structure of the C-PH does not appear to be a result of crystal-packing contacts, as there are no steric constraints on the loop with the exception of the histidine at position 256. Although this histidine residue is within van der Waals contact distance of Leu323 and His256 in a symmetry mate, it is unlikely that these weak interactions would affect the overall conformation of the loop. Since the DAPP1 and TAPP1 structures used in this comparison (Ferguson *et al.*, 2000; Thomas *et al.*, 2001) were determined in the presence of Ins(1,3,4,5)P_4 and citrate, respectively, it is likely that the conformation of the $\beta1$–$\beta2$ binding loop in the C-PH crystal structure is more representative of the conformation that this region adopts upon binding ligand. To determine how C-PH might interact with a 3-phosphoinositide such as PtdIns(3,4,5)P_3 (Zhang *et al.*, 2003; Zhang, 2005), a structural comparison of the C-PH binding loop and that of DAPP1 in complex with Ins(1,3,4,5)P_4 is presented in Fig. 6. This structural comparison illustrates that the residues implicated as being important for ligand binding in DAPP1 (Lys173, Lys182 and Arg184) are all well conserved in C-PH (Lys253, Lys262 and Arg264). These conserved residues make direct interactions with phosphates located at the 3- and 4-positions of the inositol head group. Arg257 and Arg258 in C-PH are equivalent to Leu177 and Val178 in the DAPP1 PH domain, which make two main-chain hydrogen bonds with the 5-phosphate of bound Ins(1,3,4,5)P_4 (Ferguson *et al.*, 2000). In the $\beta1$–$\beta2$ binding loop of the C-PH, Arg257 is orientated into the binding pocket and would preclude ligand binding. However, a 180° outward rotation of the main chain at Arg258 would alter the loop conformation sufficiently to permit binding

of Ins(1,3,4,5)P_4 in a similar manner to that observed in the DAPP1–Ins(1,3,4,5)P_4 structure (Ferguson *et al.*, 2000).

3.4. Comparison of N-PH and C-PH

One of the most interesting characteristics of pleckstrin is that it contains two PH domains, whereas the majority of other PH-domain-containing proteins possess only a single domain. Of the proteins containing two PH domains, pleckstrin represents the first to have both of its PH domains characterized structurally, thus permitting a comparative analysis that goes beyond primary sequence.

As with all PH domains, the overall structures of N-PH and C-PH are very similar with secondary-structure r.m.s.d.s (Å) as follows: β1, 0.49 Å; β2, 0.47 Å; β3, 0.30 Å; β4, 0.23 Å; β5, 0.64 Å; β6, 0.47 Å; β7, 0.36 Å; α1, 0.57 Å. Upon closer examination, however, the binding loops of these two domains are clearly very different (Fig. 7). Firstly, C-PH has double the positive charge within the β1–β2 phosphoinositide-binding loop compared with N-PH. Therefore, the electrostatic potential driving non-specific membrane associations would be far greater for C-PH. Secondly, with exposed valine and phenylalanine residues at positions 17 and 18, N-PH is surprisingly hydrophobic. Finally, of the three N-PH lysine residues involved in ligand binding (Lys13, Lys14 and Lys22), only Lys22 is structurally conserved in C-PH (Lys262). Together, these differences may not only contribute to differences in phosphoinositide specificity but may also result in different overall functions of these two domains within pleckstrin. Possession of two PH domains that have different phosphoinositide specificities makes pleckstrin a versatile component of phosphoinositide-based signalling pathways in platelets and may permit it to respond in distinct ways to changes in cellular levels of different phosphoinositide derivatives.

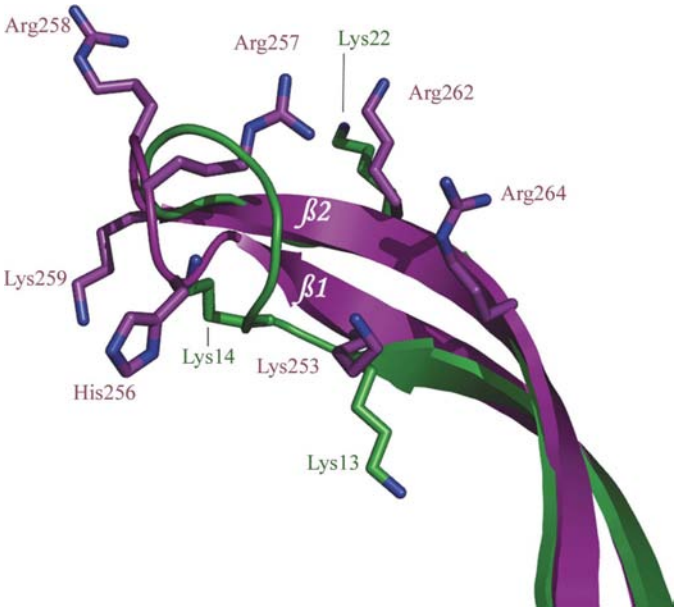

Figure 7
Structural comparison of the N- and C-terminal PH domains of pleckstrin. N-PH (green) and C-PH (purple) are illustrated using combined ribbon/stick diagrams. Residues Lys13, Lys14 and Lys22 of N-PH are comparable to residues Lys253, His256 and Lys262 of C-PH.

We would like to thank Dr Andrew Willems for critical reading of this manuscript. SGJ is a recipient of a Heart and Stroke Foundation of Canada Masters Studentship Award. This research was supported by grants to RJH and to MSJ from the Canadian Institutes of Health Research.

References

Abrams, C. S., Wu, H., Zhao, W., Belmonte, E., White, D. & Brass, L. F. (1995). *J. Biol. Chem.* **270**, 14485–14492.
Abrams, C. S., Zhang, J., Downes, C. P., Tang, X., Zhao, W. & Rittenhouse, S. E. (1996). *J. Biol. Chem.* **271**, 25192–25197.
Abrams, C. S., Zhao, W., Belmonte, E. & Brass, L. F. (1995). *J. Biol. Chem.* **270**, 23317–23321.
Abrams, C. S., Zhao, W. & Brass, L. F. (1996). *Biochim. Biophys. Acta*, **1314**, 233–238.
Auethavekiat, V., Abrams, C. S. & Majerus, P. W. (1997). *J. Biol. Chem.* **272**, 1786–1790.
Baraldi, E., Carugo, K. D., Hyvönen, M., Surdo, P. L., Riley, A. M., Potter, B. V. L., O'Brien, R., Ladbury, J. E. & Saraste, M. (1999). *Structure*, **7**, 449–460.
Brünger, A. T., Adams, P. D., Clore, G. M., DeLano, W. L., Gros, P., Grosse-Kunstleve, R. W., Jiang, J.-S., Kuszewski, J., Nilges, M., Pannu, N. S., Read, R. J., Rice, L. M., Simonson, T. & Warren, G. L. (1998). *Acta Cryst.* D**54**, 905–921.
Civera, C., Simon, B., Stier, G., Sattler, M. & Macias, M. J. (2005). *Proteins*, **58**, 354–366.
Cozier, G. E., Carlton, J., Bouyoucef, D. & Cullen, P. J. (2004). *Curr. Top. Microbiol. Immunol.* **282**, 49–88.
Craig, K. L. & Harley, C. B. (1996). *Biochem. J.* **314**, 937–942.
DeLano, W. L. (2002). *The PyMOL Molecular Graphics System.* DeLano Scientific, San Carlos, CA, USA.
Edlich, C., Stier, G., Simon, B., Sattler, M. & Muhle-Goll, C. (2005). *Structure*, **13**, 277–286.
Ferguson, K. M., Kavran, J. M., Sankaran, V. G., Fournier, E., Isakoff, S. J., Skolnik, E. Y. & Lemmon, M. A. (2000). *Mol. Cell*, **6**, 373–384.
Gailani, D., Fisher, T. C., Mills, D. C. B. & Macfarlane, D. E. (1990). *Br. J. Haematol.* **74**, 192–202.
Harlan, J. E., Hajduk, P. J., Yoon, H. S. & Fesik, S. W. (1994). *Nature (London)*, **371**, 168–170.
Haslam, R. J., Koide, H. B. & Hemmings, B. A. (1993). *Nature (London)*, **363**, 309–310.
Haslam, R. J. & Lynham, J. A. (1977). *Biochem. Biophys. Res. Commun.* **77**, 714–722.
Imaoka, T., Lynham, J. A. & Haslam, R. J. (1983). *J. Biol. Chem.* **258**, 11404–11414.
Janin, J. & Chothia, C. (1990). *J. Biol. Chem.* **265**, 16027–16030.
Jones, T. A., Zou, J. Y., Cowan, S. W. & Kjeldgaard, M. (1991). *Acta Cryst.* A**47**, 110–118.
Laskowski, R. A., MacArthur, M. W., Moss, D. S. & Thornton, J. M. (1993). *J. Appl. Cryst.* **26**, 283–291.
Lemmon, M. A. (2003). *Traffic*, **4**, 201–213.
Lyons, R. M., Stanford, N. & Majerus, P. W. (1975). *J. Clin. Invest.* **56**, 924–936.
Ma, A. D. & Abrams, C. S. (1999). *J. Biol. Chem.* **274**, 28730–28735.
McDermott, A. M. & Haslam, R. J. (1996). *Biochem. J.* **317**, 119–124.
Mayer, B. J., Ren, R., Clark, K. L. & Baltimore, D. (1993). *Cell*, **73**, 629–630.
Otwinowski, Z. & Minor, W. (1997). *Methods Enzymol.* **276**, 307–326.
Pflugrath, J. W. (1999). *Acta Cryst.* D**55**, 1718–1725.

Ponting, C. P. & Bork, P. (1996). *Trends Biochem. Sci.* **21**, 245–246.
Roll, R. L., Bauman, E. M., Bennett, J. S. & Abrams, C. S. (2000). *J. Cell Biol.* **150**, 1461–1466.
Sano, K., Takai, Y., Yamanishi, J. & Nishizuka, Y. (1983). *J. Biol. Chem.* **258**, 2010–2013.
Sloan, D. C., Wang, P., Bao, X. & Haslam, R. J. (2002). *Biochem. Biophys. Res. Commun.* **293**, 640–646.
Smith, C. I., Islam, K. B., Vorechovsky, I., Olerup, O., Wallin, E., Rabbani, H., Baskin, B. & Hammerstrom, L. (1994). *Immunol. Rev.* **138**, 159–183.
Thomas, C. C., Dowler, S., Deak, M., Alessi, D. R. & van Aalten, D. M. F. (2001). *Biochem. J.* **358**, 287–294.
Tyers, M., Haslam, R. J., Rachubinski, R. A. & Harley, C. B. (1989). *J. Cell. Biochem.* **40**, 133–145.
Tyers, M., Rachubinski, R. A., Sartori, C. S., Harley, C. B. & Haslam, R. J. (1987). *Biochem. J.* **243**, 249–253.
Tyers, M., Rachubinski, R. A., Stewart, M. I., Varrichio, A. M., Shorr, R. G. L., Haslam, R. J. & Harley, C. B. (1988). *Nature (London)*, **333**, 470–473.
Vagin, A. & Teplyakov, A. (1997). *J. Appl. Cryst.* **30**, 1022–1025.
Yoon, H. S., Hajduk, P. J., Petros, A. M., Olejniczak, E. T., Meadows, R. P. & Fesik, S. W. (1994). *Nature (London)*, **369**, 672–675.
Zhang, Y. (2005). PhD thesis. McMaster University, Canada.
Zhang, Y., Bao, X. & Haslam, R. J. (2003). *FASEB J.* **17**, A171.